BASIC RESEARCH STUDIES

Long-term patency of small-diameter vascular graft made from fibroin, a silk-based biodegradable material

Soichiro Enomoto, MD, PhD,[a] Makoto Sumi, MD, PhD,[a,b] Kan Kajimoto, MD, PhD,[c]
Yasumoto Nakazawa, PhD,[d] Rui Takahashi, MS,[d] Chiyuki Takabayashi, PhD,[e] Tetsuo Asakura, PhD,[d] and
Masataka Sata, MD, PhD,[f] *Tokyo, Nagano, and Tokushima, Japan*

Objective: There is an increasing need for vascular grafts in the field of surgical revascularization. However, smaller vascular grafts made from synthetic biomaterials, particularly those <5 mm in diameter, are associated with a high incidence of thrombosis. Fibroin is a biodegradable protein derived from silk. Silk fibroin from *Bombyx mori* provides an antithrombotic surface and serves as a scaffold for various cell types in tissue engineering. We evaluated the potential of fibroin to generate a vascular prosthesis for small arteries.
Methods: A small vessel with three layers was woven from silk fibroin thread. These fibroin-based grafts (1.5 mm diameter, 10 mm length) were implanted into the abdominal aorta of 10- to 14-week-old male Sprague-Dawley rats by end-to-end anastomosis. Polytetrafluoroethylene (PTFE)-based grafts were used as the control. To investigate the origin of the cells in the neointima and media, bone marrow transplantation was performed from green fluorescent protein (GFP) rats to wild-type rats.
Results: The patency of fibroin grafts at 1 year after implantation was significantly higher than that of PTFE grafts (85.1% vs 30%, *P* < .01). Endothelial cells and smooth muscle cells (SMCs) migrated into the fibroin graft early after implantation and became organized into endothelial and medial layers, as determined by anti-CD31 and anti-α-smooth muscle actin immunostaining. The total number of SMCs increased 1.6-fold from 1 month to 3 months. Vasa vasorum also formed in the adventitia. Sirius red staining of the fibroin grafts revealed that the content of collagen significantly increased at 1 year after implantation, with a decrease in fibroin content. GFP-positive cells contributed to organization of a smooth muscle layer.
Conclusions: Small-diameter fibroin-based vascular grafts have excellent long-term patency. Bone marrow-derived cells contribute to vascular remodeling after graft implantation. Fibroin might be a promising material to engineer vascular prostheses for small arteries. (J Vasc Surg 2010;51:155-64.)

Clinical Relevance: The present study evaluated the efficacy of a fibroin, a new silk-based biodegradable material, to generate small diameter grafts. When implanted in rat abdominal aorta, a fibroin-based graft (1.5 mm in diameter) showed excellent long-term patency, with optimal mechanical properties. Endothelial cells and smooth muscle cells migrated into the fibroin graft early after implantation and became organized into endothelial and medial layers, generating a vascular-like structure. Our findings suggest that a silk fibroin might be a promising material to develop vascular prostheses for smaller arteries.

Small-diameter prostheses are needed for peripheral revascularization procedures.[1] Autologous saphenous vein is considered the material of choice for bypass grafts to relieve symptoms or avoid amputation in patients with peripheral arterial occlusive disease. Many patients who require a lower-limb bypass graft have no available good-quality vein for the procedure and thus require a prosthetic graft.[2] However, smaller vascular grafts made from conven-

155

tional synthetic biomaterials, such as expanded polytetra-fluoroethylene (ePTFE) and polyethylene terephthalate (Dacron), particularly those <5 mm in internal diameter, are associated with a high incidence of thrombosis, especially when the distal anastomosis is below the knee.[3]

To overcome these limitations, various tissue-engineered vascular grafts have been developed.[4] The utility and clinical experience of these new grafts have been reported.[5-9] The most promising approach was described by L'Heureux et al,[7,8] who developed a completely autologous technique called sheet-based tissue engineering. Autologous tissue-engineered vascular grafts have been implanted as arteriovenous shunts in 10 patients with end-stage renal disease. In five patients, the grafts were functioning for hemodialysis at 6 to 20 months after implantation.[9] Despite these encouraging initial results, this method takes a long time, about 24 days, and thus cannot be applied for emergency surgery.

Silk has been used in biomedical applications for centuries, primarily for suturing. Silk fibers are composed primarily of two types of proteins: (1) sericin, the antigenic gum-like protein surrounding the fibers, and (2) fibroin, the core filaments of silk consisting of highly organized β-sheet crystal regions and semicrystalline regions responsible for silk's elasticity compared with fibers of similar tensile integrity.[10] If sericin is removed, the biologic responses to the core fibroin fibers appear to be comparable with the responses to most other commonly used biomaterials. Furthermore, silk is susceptible to proteolytic degradation in vivo and is absorbed slowly.[11-14]

Fibroin provides an antithrombotic surface and serves as a scaffold for various cell types in tissue engineering. Silk fibroin offers versatility in matrix scaffold design for engineering of a variety of tissues in which mechanical performance and biologic interactions are required, such as bone, ligaments, tendons, blood vessels, and cartilage.[15-18]

In the present study, we created a small-diameter biodegradable fibroin-based graft with optimal mechanical properties and evaluated its in vivo patency, cellularization, and degradation in the rat arterial circulation for up to 18 months. We also examined the participation of bone marrow (BM)-derived cells in the formation of a vascular-like structure in the implanted prosthesis. Our findings suggest that silk fibroin might be a promising material to develop vascular prostheses for smaller arteries.

MATERIALS AND METHODS

Fabrication of silk fibroin vascular graft. Artificial blood vessels were made by a combination of plaiting of silk fibers and winding of cocoon filaments on a round sectional core, which was a vinyl chloride rod. To produce artificial blood vessels by this method, 36 thin silk threads (14 denier/thread) were first plaited together. After that, three or four cocoon filaments (1.6 to 1.8 denier/filament) were reeled around the plaited silk fibers. The combination of plaiting of silk fibers and winding of cocoon filaments was performed two or more times.

A degumming process was used to remove the water-soluble sericin component. The tube was dipped in a fibroin solution to make the fibroin filaments stick together, dried, and fixed in ethanol, and the cocoon filament vessel was removed from the central core. This material was left under heat (>80°C) in water so that the cocoon filament vessel could be easily separated from the central core. Thus, an artificial blood tube with a 1.5-mm inner diameter made from cocoon filaments was produced.

Animals. Male Sprague-Dawley (SD) rats weighing 400 to 500 g were purchased from SLC (Shizuoka, Japan). Transgenic rats (SD background) that ubiquitously express enhanced green fluorescent protein (GFP) were donated by Dr Masaru Okabe (Osaka University, Osaka, Japan).[19] All rats were kept in microisolator cages with a 12-hour light/dark cycle. All experimental procedures and protocols were approved by the Animal Care and Use Committee of the University of Tokyo and complied with the *Guide for the Care and Use of Laboratory Animals* (National Institutes of Health publication No. 86-23, revised 1985).

Surgical procedure. A silk fibroin graft (10 mm long, 1.5 mm inner diameter) was implanted into the rat abdominal aorta, which had a diameter of about 1.5 mm. Rats were anesthetized with an intraperitoneal injection of pentobarbital (50 mg/kg body weight). The abdominal aorta was exposed and the aortic branches in this segment were ligated.

After an intravenous injection of heparin (100 IU/kg), the proximal and distal portions of the infrarenal aorta were clamped. A 10-mm segment of aorta was removed and replaced by a fibroin graft by end-to-end anastomosis using interrupted 9-0 monofilament nylon sutures (BEAR, Japan), starting with two stay sutures at 180° to each other, then suturing the front wall, followed by the back wall. Each anastomosis required 10 to 12 stitches. The distal, then the proximal vascular clamps were slowly removed, and flow was restored through the fibroin graft. Total ischemia time was 30 to 60 minutes.

A small tube made of polytetrafluoroethylene (PTFE), 1.5 mm in diameter (HAGITEC, Chiba, Japan), was implanted into the rat abdominal aorta in the same manner.

Graft patency was confirmed visually. No anticoagulants or antiplatelet agents were administered postoperatively. Two animals died from surgical complications, such as bleeding from the site of anastomosis, and were not included in this study.

Graft patency was monitored by color Doppler imaging and pulse waves recorded with a 12-MHz sector probe and an echo-imaging apparatus (EnVisor M2540A, Phillips, Tokyo) at 2, 4, 8, 12, 24, 48, and 72 weeks, under anesthesia with pentobarbital. Graft diameter and blood flow velocity were measured. Signs of thrombosis and aneurysm formation were carefully checked. Angiography was performed before sacrifice by injection of 1 mL contrast material (Hexabrix 320, Guerbet, France), and blood flow was assessed using a C-arm digital fluoroscopy system (Sirus Power/C, Hitachi Medico, Tokyo, Japan).

Histologic examination. Three to five animals were killed with an overdose of pentobarbital at 2, 4, 12, 24, 48, and 72 weeks. Before euthanasia, rats underwent a general physical examination to evaluate their condition. At death, the rats were perfused with 0.9% saline solution through the left ventricle.

The grafts were carefully removed with surrounding tissue, cut transversely in the midline into two pieces, and fixed in methanol or snap-frozen in OCT compound (Tissue-Tek, Tokyo) for histologic analyses. Methanol-fixed samples were embedded in paraffin. Paraffin-embedded sections (4-μm thick) were processed for hematoxylin and eosin staining.

Immunohistochemical staining was performed as previously reported.[20] The sections were incubated with primary antibodies, including alkaline phosphatase-conjugated anti-α-smooth muscle actin (SMA; clone 1A4, Sigma-Aldrich, St. Louis, Mo), anti-rat CD31 (clone TLD-3A12, BD Biosciences, San Jose, Calif), or anti-CD68 (clone ED1, Serotec, Oxford, United Kingdom), followed by incubation with biotinylated anti-mouse immunoglobulin (Ig) G secondary antibody (DAKO, Glostrup, Denmark) and subsequent use of the avidin-biotin complex technique and Vector Red substrate (Vector Laboratories, Burlingame, CA). Nuclei were counterstained with hematoxylin.

Sirius red polarization method for collagen staining. Sirius red polarization microscopy was performed, as described previously, to visualize interstitial collagen and fibroin.[21] Fresh frozen sections (5 μm) were rinsed with distilled water and incubated with 0.1% Sirius red (Sigma-Aldrich) in saturated picric acid for 90 minutes. Sections were rinsed twice with 0.03 N HCl for 1 minute each time and then immersed in distilled water. After dehydration with 70% ethanol for 30 seconds, the sections were coverslipped. The stained sections were examined under a polarization microscope (Eclipse LV100POL, Nikon, Tokyo). Images were digitized with a CCD camera (Digital Sight DS-2Mv, Nikon). As the fiber thickness increases, the color changes from green to red.

BM transplantation. To keep track of bone marrow (BM)-derived cells in the process of graft remodeling, we performed BM transplantation (BMT) from GFP rats to wild-type SD rats, as described previously.[20,22] BM cells were harvested from the femurs and tibias of GFP rats. Eight-week-old male wild-type rats were lethally irradiated with a total dose of 15 Gy (MBR-1520RB, Hitachi). One day later, the recipient rats received unfractionated BM cells (3×10^7) suspended in 1 mL phosphate-buffered saline by tail vein injection. Peripheral leukocytes (80% to 90%) had been reconstituted as determined by flow cytometry. We confirmed >80% bone marrow chimerism.[23] At 4 to 16 weeks after BMT, fibroin grafts were implanted into the chimeric rats.

Cell culture. BMCs were harvested from the femurs and tibias of donor rats as described previously.[23] For BMC seeding, fibroin sheets (1×1 cm) were placed in a 24-well plate. Cells were seeded onto the fibroin sheets (5×10^6 cells/well) by direct pipetting and incubated in 1 mL Dulbecco modified Eagle medium supplemented with 10% fetal bovine serum, 50 U/mL penicillin, and 50 μg/mL streptomycin at 37°C in 5% carbon dioxide for 7 days. The cell culture medium was changed every 4 days. At 7 days, the seeded fibroin sheets were gently washed in phosphate buffered saline and fixed for scanning electron microscopic study.

Scanning electron microscopy. Samples were fixed in 2% paraformaldehyde and 2.5% glutaraldehyde, and then postfixed in 1% osmium tetroxide and dehydrated in a graded series of ethanol. After critical point drying, samples were sputter coated with a thin layer of platinum/palladium and analyzed with a scanning electron microscope (S-3500N, Hitachi, Tokyo).

Double-immunofluorescence study. Frozen sections were incubated with anti-GFP rabbit polyclonal antibody (Molecular Probes, A11122, Eugene, Ore) and a cell-specific primary antibody (Cy3-conjugated anti-αSMA [Sigma-Aldrich], anti-rat CD31 [BD Biosciences], anti-CD45 [clone sc-1178, Santa Cruz Biotechnology, Santa Cruz, Calif] or biotinylated anti-SM1 antibody [clone KM3669, Kyowa Hakko Kogyo, Tokyo]). Alexa Fluor 488-labeled anti-rabbit IgG antibody (Molecular Probes) and Cy3-conjugated anti-mouse antibody (Jackson ImmunoResearch, West Grove, Pa) or Cy3-conjugated streptavidin (Jackson ImmunoResearch) were used to visualize the distribution of primary antibodies. Nuclei were counterstained with Hoechst 33258 (Sigma-Aldrich). The sections were observed under a confocal microscope (FLUOVIEW FV300, Olympus, Tokyo).

Statistics. Data are presented as mean ± standard error of the mean. Comparisons of means were performed by one-way analysis of variance, followed by the Sheffe post hoc test. Graft patency for each group was determined by Kaplan-Meier analysis. The log-rank test was used to test for differences between the groups. Statistical significance was defined as $P < .05$.

RESULTS

Small-diameter vascular graft made of silk fibroin and its biocompatibility. A 1.5 mm-diameter vascular graft was fabricated from fibroin fibers (Fig 1, *A* and *B*). Bone marrow cells (BMCs) from SD rats were seeded and cultivated on the graft. Scanning electron microscopy demonstrated that BMCs attached, differentiated, and coated the surface of the graft at 7 days (Fig 1, *C* and *D*). To assess the efficacy of fibroin-based grafts in vivo, a 1.5-mm-diameter vascular graft made of fibroin was implanted into the infrarenal abdominal aorta of a SD rat by end-to-end anastomosis (Fig 1, *E* and *F*). The patency of the graft was examined by ultrasound Doppler flow studies every 2 weeks, which revealed a flow signal in the graft, without aneurysmal dilation (Fig 1, *G, upper panel*). Pulsed-wave Doppler ultrasound imaging confirmed blood flow through the patent graft (Fig 1, *G, lower panel*). Angiography showed no aneurysmal dilation (Fig. 1, *H*).

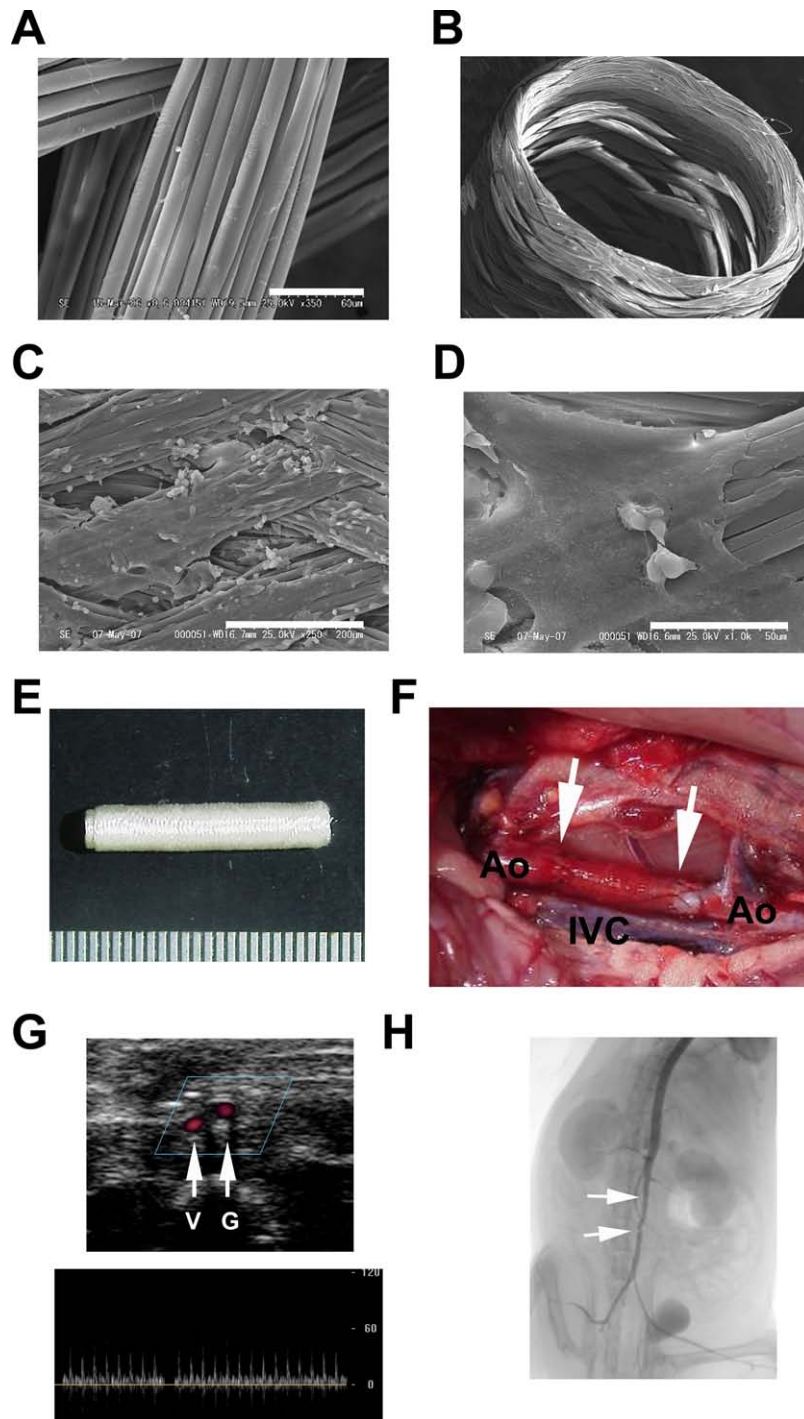**Histologic changes in implanted fibroin graft.** Histologic analysis showed cellular intimal thickening and

Fig 1. A, Scanning electron microscopic (SEM) image shows silk fibroin filaments after removal of sericin proteins (*scale bar,* 60 μm). **B,** A small artificial vascular graft was made from fibroin fibers. **C and D,** Attachment and differentiation of bone marrow cells (BMCs) on fibroin graft. Rat BMCs were isolated as described previously. At 7 days after seeding, BMCs had spread and grown on the fibroin graft, forming cell sheets with a possible extracellular matrix (**C,** *scale bar,* 200 μm; **D,** *scale bar,* 50 μm). **E,** The fibroin-based graft (1.5 mm internal diameter) was implanted into rat abdominal aorta by end-to-end anastomosis **(F).** The *arrows* indicate anastomosis sites. *Scale,* 1 mm. *Ao,* Aorta; *IVC,* inferior vena cava. **G,** Blood flow within the graft was monitored by **(upper panel)** color Doppler imaging and **(lower panel)** pulse wave velocity measurement. **H,** Angiography revealed a patent fibroin graft. The *arrows* indicate anastomotic sites. *G,* Graft; *V,* inferior vena cava.
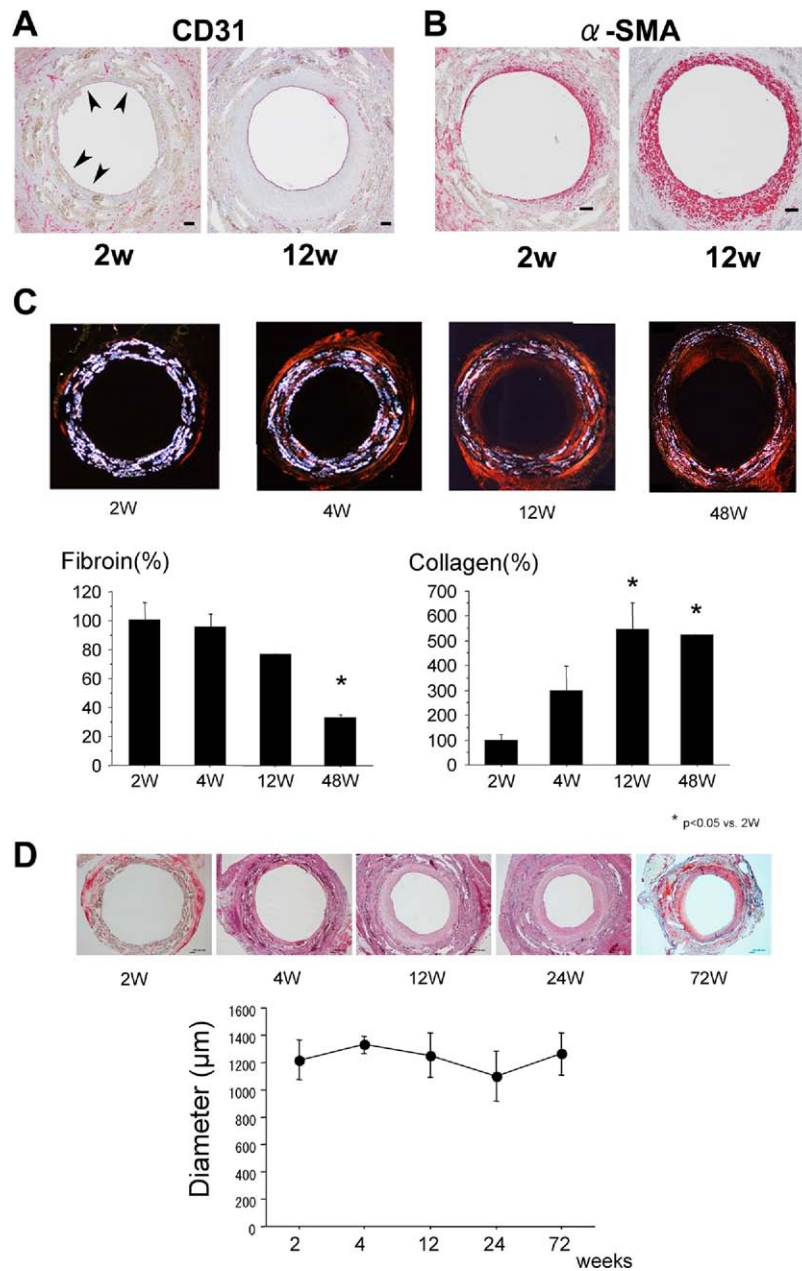
Fig 2. A, Cross-sections of fibroin grafts at 2 and 12 weeks after implantation stained with anti-CD31 antibody (*scale bar,* 100 μm). Endothelial cell coverage was partial at 2 weeks after implantation. The *arrowheads* indicate CD31-positive endothelial cells. At 12 weeks after implantation, most of the luminal surface of the fibroin grafts was covered by endothelial cells. **B,** Anti-α-smooth muscle actin (α-*SMA*) immunostaining of fibroin grafts was performed at 2 and 12 weeks after implantation (*scale bar,* 100 μm). The thickness of the α-SMA-positive cell layer gradually increased. The newly formed media-like structure within the fibroin graft was highly cellular with α-SMA-positive cells. **C,** Polarization microscopic images of fibroin grafts after Sirius red staining. The content of fibroin *(white)* gradually decreased, while collagen *(red)* content increased after implantation (*$P < .05$ vs 2 weeks). The *error bars* indicate the standard error of the mean. **D,** The internal diameter of the fibroin graft was measured. The diameter remained unchanged.

infiltration of cells into the fibroin graft. Anti-CD31 immunostaining of the fibroin graft revealed partial endothelial cell coverage (20.6% ± 9.5%) at 2 weeks after implantation (Fig 2, *A*). At 12 weeks, CD31-positive cells covered 92.2% ±

2.4% of the luminal surface in the fibroin graft. Anti-α-SMA immunostaining revealed that a layer of SMCs was formed along the fibroin graft at 2 weeks (Fig 2, *B*). The α-SMA-positive cell layer was thickened at 12 weeks.

We used Sirius red staining to evaluate biodegradability and extracellular matrix deposition of the fibroin graft. Polarization microscopy showed that the content of fibroin was decreased at 48 weeks after implantation (32.9% ± 1.9%, $P < .05$ vs 2 weeks; Fig 2, *C*). On the other hand, the collagen content was markedly increased at 12 weeks (544.9% ± 104.2%, $P < .05$ vs 2 weeks) and 48 weeks. Histologic analysis showed no aneurysmal dilatation at any time point (Fig 2, *D*). The graft diameter remained unchanged up to 1 year after implantation. The grafts were patent without luminal narrowing.

Excellent long-term patency of fibroin graft. The patency of the 27 fibroin grafts and the 10 PTFE grafts were compared (Fig 3, *A*). Four of the 10 PTFE grafts were occluded ≤4 weeks, and one graft was occluded at 12 weeks. In contrast, only three of 27 fibroin grafts became occluded. The overall 1-year patency of fibroin grafts was 85.0%, which was significantly higher than that of PTFE grafts. Histologic analysis revealed that cells migrated to the fibroin grafts and covered the luminal side completely (Fig 3, *B*); however, no cell attachment occurred on PTFE grafts (Fig 3, *C*). Thrombus formation was observed within the occluded PTFE grafts.

Organization of vessel-like structure at 1 year after fibroin graft implantation. Macroscopic observation of the implanted fibroin graft at 1 year confirmed a smooth luminal surface with no signs of thrombus or aneurysmal dilatation (Fig 4, *A*). Histologic analysis of the fibroin grafts showed formation of an endothelial layer and a media-like smooth muscle layer (Fig 4, *B*). Vasa vasorum had also formed in the adventitia. Anti-CD68 immunostaining revealed substantial infiltration of macrophages and phagocytic phenomena around the remnants of fibroin. These findings indicate that organization of a vessel-like structure could occur at 1 year using a fibroin graft as a scaffold.

Origin of endothelial cells and SMCs that accumulated along the graft. Fibroin grafts were implanted in the BMT rats whose BM cells had been reconstituted by those from GFP rats. At 12 weeks after surgery, GFP-positive cells accumulated in the fibroin grafts (Fig 5, *A*). GFP-positive cells that were also positive for α-SMA and SM1 were readily detected (Fig 5, *A* and *B*). The total number of SM1-positive cells in grafts gradually increased from 119.0 ± 19.9/section at 1 month to 166.9 ± 29.5/section at 3 months (Fig 5, *C*). A significant percentage of SM1-positive cells expressed GFP (65.9% ± 4.3% at 1 month; 50.9% ± 4.9% at 3 months; Fig 5, *C*). These data suggest that BM-derived cells substantially contribute to the formation of the SMC layer in the graft in the early phase. On the other hand, a few BM-derived cells were positive for CD31 in the luminal layer. Few CD45-positive cells were observed in the smooth muscle layer or on the luminal side.

DISCUSSION

In this study, we evaluated the potential of fibroin to generate a vascular prosthesis for small arteries. A small
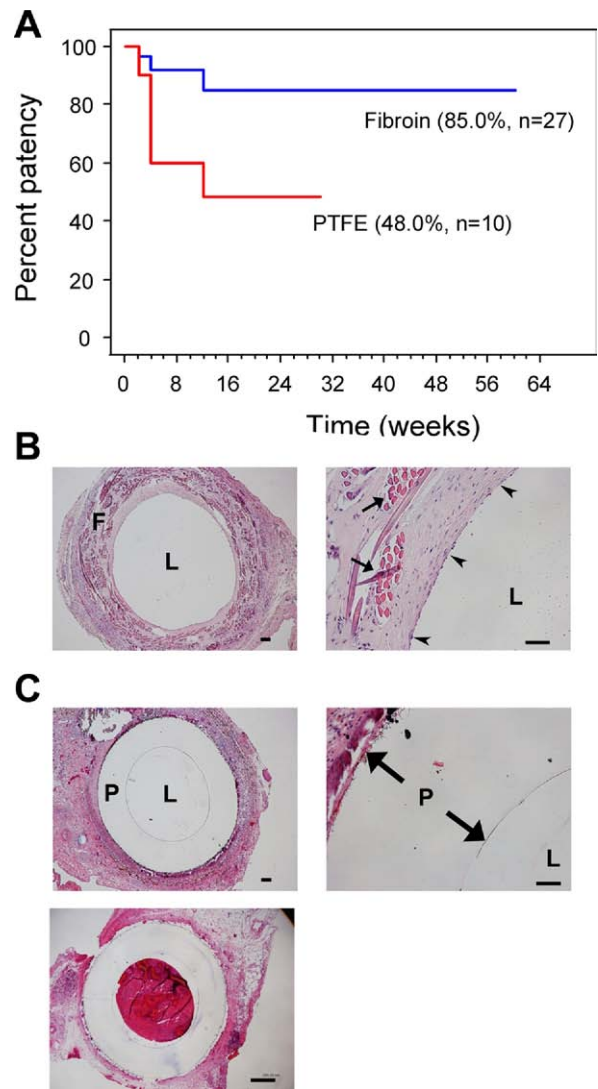

Fig 3. **A,** Kaplan-Meier analysis shows graft patency for 27 fibroin and 10 polytetrafluoroethylene (PTFE) grafts implanted into rat aortas at 2, 4, 8, 12, 24, 48, and 72 weeks (see text for details). **B,** Histologic analysis of fibroin grafts. **Left,** Cross section of the fibroin graft at 4 weeks after implantation (hematoxylin and eosin staining; *scale bar,* 100 μm). Cells migrated to the fibroin grafts and covered the luminal side completely. *F,* Fibroin graft. *L,* lumen. **Right,** The *arrowheads* indicate media-like layer and endothelium-like layer, and the *arrows* indicate fibroin fibers (*scale bar,* 50 μm). **C,** Histological analysis of PTFE *(P)* grafts. **Left,** Cross section of the PTFE graft at 4 weeks after implantation (hematoxylin and eosin staining staining; *scale bar,* 100 μm). *L,* Lumen. **Right,** Very few cells attached on the luminal side of PTFE graft (*scale bar,* 50 μm). **Bottom,** Thrombus formation in the occluded PTFE graft (*scale bar,* 250 μm).

artificial vessel with three layers was woven from fibroin thread. Fibroin-based grafts were implanted into the abdominal aorta of rats by end-to-end anastomosis. The patency rate of fibroin grafts at 1 year after implantation was
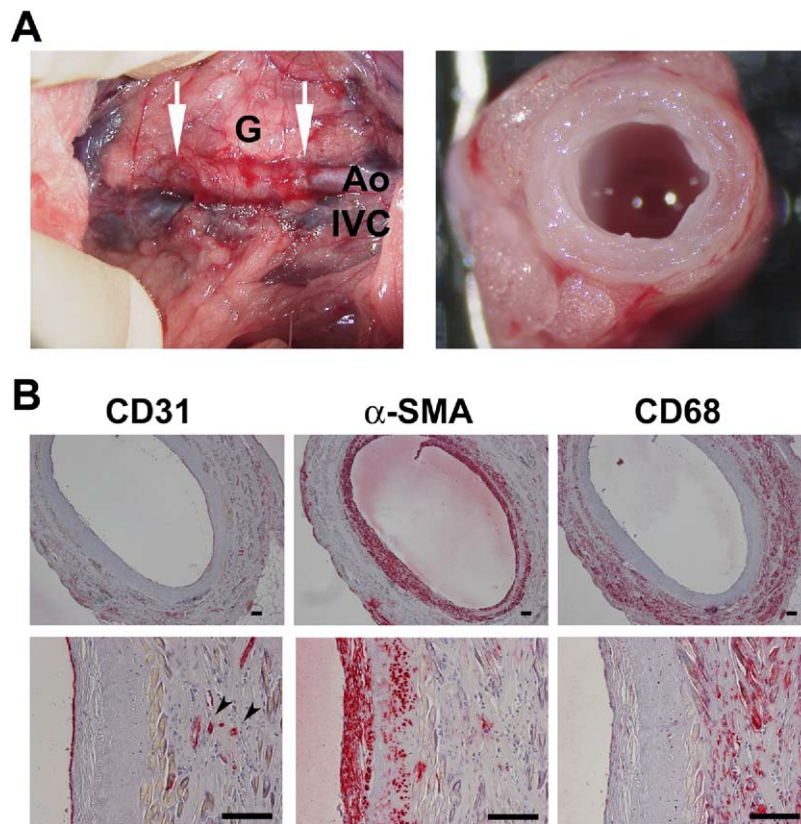
Fig 4. A, Macroscopic image of implanted fibroin graft *(G)* at 1 year shows no aneurysm formation. The *arrows* indicate anastomotic sites. The fibroin grafts appeared to be integrated into the surrounding tissue and showed no signs of thrombosis, stenosis, or mechanical failure. *Ao,* Aorta; *IVC,* inferior vena cava. **B,** Histologic analysis of the fibroin graft at 1 year showed a confluent endothelial layer and smooth muscle cell layers, as determined by immunostaining against CD31 and α-smooth muscle actin *(α-SMA)*, respectively. Immunostaining for CD68 revealed substantial macrophage infiltration in the adventitia. Formation of vasa vasorum was noted *(arrowheads)*. *Scale bar*, 100 μm (upper and lower panels).

significantly higher than that of PTFE grafts. Endothelial cells and SMCs migrated into the fibroin graft early after implantation and became organized into an endothelium and a media-like smooth muscle layer. BM-derived cells substantially contributed to organization of the smooth muscle layer, but not to endothelium formation.

There is an increasing need for vascular grafts in the field of surgical revascularization. However, smaller vascular grafts made from synthetic biomaterials, particularly those <5 mm in diameter, are associated with a high incidence of thrombosis. Fibroin is a biodegradable protein derived from silk that provides an antithrombotic surface and serves as an ideal scaffold for various cell types in tissue engineering.[17]

Cell attachment, migration, proliferation, and differentiation on biomaterials are critical elements for successful tissue regeneration.[24] In the present study, BMCs were shown to attach, spread, and proliferate on the silk fiber matrix. When a fibroin graft was implanted in the rat abdominal aorta, endothelial cells and SMCs were organized into a vessel-like structure. The luminal surface of the graft was almost completely covered by a layer of endothe-

lial cells by 12 weeks. Scanning electron microscopy documented the endothelial integrity of the luminal surface of the fibroin grafts. Immunohistochemical examination also showed newly organized endothelium of the fibroin grafts. It is well known that endothelialization yields antithrombogenic properties.[25,26]

Most of the fibroin grafts were free of thrombus formation during the study's observation period. SMCs accumulated and formed a media-like structure. In addition, we found that vasa vasorum-like capillaries developed around the fibroin grafts, suggesting that the newly developed vessel-like structure can receive a physiologic blood supply for the maintenance of vascular homeostasis.

It is critical that the material for a vascular conduit can be sutured and has sufficient burst strength to withstand physiologic blood pressure. Biodegradable scaffolds to establish tissue-engineered vascular autografts have been used for lower-pressure circulation, but not for the arterial system.[27] Recently, we and others reported that fibroin fiber can produce strong and tough fibers.[10,15,28,29] The stress-strain curve revealed that the Young's modulus of the
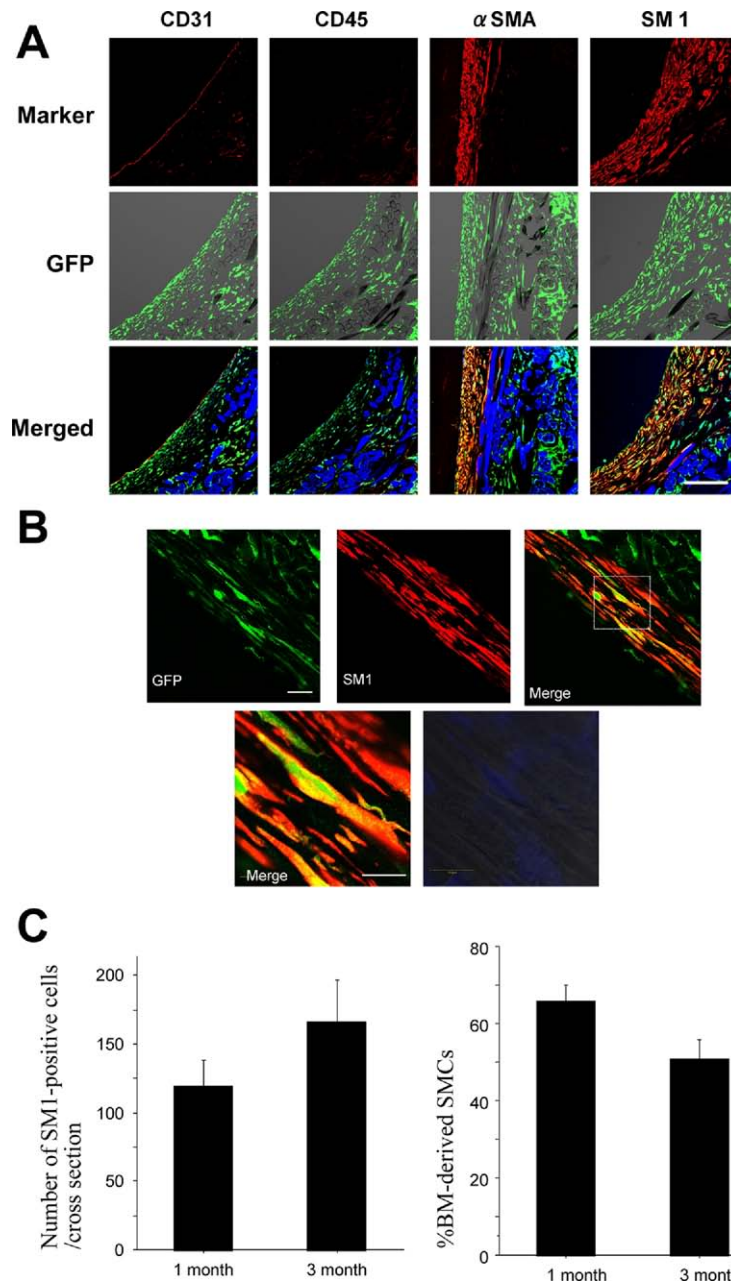
Fig 5. A, At 4 to 16 weeks after BMT from GFP rats to wild-type SD rats, fibroin grafts were implanted into the chimeric rats. Fibroin grafts transplanted in BMT rats were snap-frozen at 4 or 12 weeks. Nuclei were counterstained with Hoechst 33258 *(blue)*. We readily detected GFP-positive cells *(green)* that were positive for α-SMA or SM1 *(red)*. There were few GFP and CD31 *(red)* double-positive cells. Few CD45-positive cells *(red)* were observed within the newly formed vessel wall-like structure. *Scale bar,* 100 μm. **B,** Representative images of BM-derived smooth muscle-like cells on fibroin graft at 12 weeks after implantation into BMT rat. Frozen sections were stained for GFP *(green)* and SM1 *(red)*. The *arrows* indicate double-positive cells. *Scale bar,* 20 μm. Lower panels are higher magnification images of the media-like layer. The lower right panel shows a differential interference contrast microscopic image with nuclei *(blue)*. *Scale bar,* 10 μm. **C,** Frequency of GFP- and SM1-positive cells in the media-like structure of fibroin grafts was measured at 1 and 3 months after implantation. The *error bars* indicate the standard error of the mean.

native *Bombyx mori* silk fibroin fiber was 5.0 Gpa, with a remarkable combination of strength and toughness.[29] We found that ultimate tensile strength of the fibroin fiber was >320 MPa and that strain at break was >20%.[29]

Consistently, neither rupture nor aneurysm formation was observed when a small-diameter vascular graft made from fibroin was implanted into rat abdominal aorta in the present study. Histologic analysis demonstrated that the

diameter of the fibroin grafts remained unchanged for up to 18 months. Sirius red staining showed that collagen fibers were deposited within the fibroin graft along with smooth muscle accumulation. Sufficient collagen accumulation can act as a framework and strengthen the graft against high systemic pressure while the fibroin grafts are gradually absorbed. It is critical for biodegradable materials to maintain sufficient strength until the newly formed organ becomes mechanically and physiologically mature. If degradation is too fast before the vessel is organized, rupture or aneurysm formation potentially occurs. Gradual proteolytic degradation takes longer in silk[11-14]: silk fibers generally lose most of their tensile strength ≤1 year in vivo and become unrecognized at the site ≤2 years.

An adequate inflammatory response seems to be required for the degradation of silk. Systematic in vivo studies indicate that silk induces a foreign body response comparable to that of most commonly used degradable synthetic and natural polymers, such as polyglycolic acid-poly lactic acid copolymers and collagen.[15,30] Similarly, we observed that the content of fibroin was significantly decreased at 1 year after implantation. In abdominal wound closure in rats, silk promoted a moderate foreign body response compared with monofilament and multifilament nylon and polyglycolic acid sutures.[31] In our study, macrophages accumulated around the fibroin grafts at 1 year after implantation. Few inflammatory cells infiltrated within the newly formed vessel wall.

We and others previously reported that BM can give rise to vascular cells that participate not only in repair but also in lesion formation after injury of the vessel wall.[20,22,32] On the other hand, other authors reported that BMCs do not participate substantially in vascular remodeling in some experimental systems.[33,34] These BM-derived vascular cells are considered to be endothelial-like progenitor cells or smooth muscle-like progenitor cells.[35,36] In the present study, a significant number of SMCs were observed in the media-like structure derived from BMCs in the implanted fibroin graft. Some BM-derived cells expressed not only α-SMA but also SM1, a marker for highly differentiated SMC.

We previously reported that the contribution of BMCs to arterial remodeling in mice depends on the type of vascular injury.[22,23] BMCs would substantially contribute to lesion formation when arteries are subjected to severe injury that kills most endothelial and medial cells. We speculate that BM-derived cells were recruited to repair the implanted vascular prosthesis because not enough local mesenchymal cells were available for the process. After graft implantation, smooth muscle-like progenitor cells were recruited and accumulated along the graft. It is likely that endothelial cells migrated from the adjacent endogenous vessel wall.

In this study, we used rat abdominal model to implant fibroin graft. There are several differences in vascular biology and coagulation activity between rodents and humans. Apparently, there are many limitations to extrapolate data in this study to clinical use of the vascular prosthesis.[37]

Clinical feasibility of the graft should be evaluated carefully with preclinical studies using other models with vascular biology more similar to that of man.[38]

CONCLUSIONS

Our findings suggest that silk-based fibroin grafts provide excellent patency when implanted in smaller vessels. The fibroin graft gradually degraded with formation of an artery-like structure by endogenous endothelial cells and SMCs. Fibroin may hold the promise to generate vascular prostheses for smaller-diameter arteries.

AUTHOR CONTRIBUTIONS

Conception and design: SE, TA, MS
Analysis and interpretation: SE, MS, KK, YN, RT, CT
Data collection: SE, MS, KK, YN, RT, CT
Writing the article: SE, MS, YN, RT, CT, TA, MS
Critical revision of the article: SE, TS, MS
Final approval of the article: SE, MS, KK, YN, RT, CT, TA, MS
Statistical analysis: SE, MS
Obtained funding: TA, MS
Overall responsibility: MS

REFERENCES

1. Pektok E, Nottelet B, Tille JC, Gurny R, Kalangos A, Moeller M, et al. Degradation and healing characteristics of small-diameter poly(epsilon-caprolactone) vascular grafts in the rat systemic arterial circulation. Circulation 2008;118:2563-70.
2. Daenens K, Schepers S, Fourneau I, Houthoofd S, Nevelsteen A. Heparin-bonded ePTFE grafts compared with vein grafts in femoro-popliteal and femorocrural bypasses: 1- and 2-year results. J Vasc Surg 2009;49:1210-6.
3. Pawlowski KJ, Rittgers SE, Schmidt SP, Bowlin GL. Endothelial cell seeding of polymeric vascular grafts. Front Biosci 2004;9:1412-21.
4. Langer R, Vacanti JP. Tissue engineering. Science 1993;260:920-6.
5. Sharp MA, Phillips D, Roberts I, Hands L. A cautionary case: the SynerGraft vascular prosthesis. Eur J Vasc Endovasc Surg 2004;27:42-4.
6. Shin'oka T, Matsumura G, Hibino N, Naito Y, Watanabe M, Konuma T, et al. Midterm clinical result of tissue-engineered vascular autografts seeded with autologous bone marrow cells. J Thorac Cardiovasc Surg 2005;129:1330-8.
7. L'Heureux N, Dusserre N, Konig G, Victor B, Keire P, Wight TN, et al. Human tissue-engineered blood vessels for adult arterial revascularization. Nat Med 2006;12:361-5.
8. L'Heureux N, McAllister TN, de la Fuente LM. Tissue-engineered blood vessel for adult arterial revascularization. N Engl J Med 2007; 357:1451-3.
9. McAllister TN, Maruszewski M, Garrido SA, Wystrychowski W, Dusserre N, Marini A, et al. Effectiveness of haemodialysis access with an autologous tissue-engineered vascular graft: a multicentre cohort study. Lancet 2009;373:1440-6.
10. Altman GH, Diaz F, Jakuba C, Calabro T, Horan RL, Chen J, et al. Silk-based biomaterials. Biomaterials 2003;24:401-16.
11. Lam KH, Nijenhuis AJ, Bartels H, Postema AR, Jonkman MF, Pennings AJ, et al. Reinforced poly(L-lactic acid) fibres as suture material. J Appl Biomater 1995;6:191-7.
12. Rossitch E, Jr., Bullard DE, Oakes WJ. Delayed foreign-body reaction to silk sutures in pediatric neurosurgical patients. Childs Nerv Syst 1987;3:375-8.
13. Salthouse TN, Matlaga BF, Wykoff MH. Comparative tissue response to six suture materials in rabbit cornea, sclera, and ocular muscle. Am J Ophthalmol 1977;84:224-33.

14. Soong HK, Kenyon KR. Adverse reactions to virgin silk sutures in cataract surgery. Ophthalmology 1984;91:479-83.

15. Altman GH, Horan RL, Lu HH, Moreau J, Martin I, Richmond JC, et al. Silk matrix for tissue engineered anterior cruciate ligaments. Biomaterials 2002;23:4131-41.

16. Inouye K, Kurokawa M, Nishikawa S, Tsukada M. Use of Bombyx mori silk fibroin as a substratum for cultivation of animal cells. J Biochem Biophys Methods 1998;37:159-64.

17. Minoura N, Aiba S, Gotoh Y, Tsukada M, Imai Y. Attachment and growth of cultured fibroblast cells on silk protein matrices. J Biomed Mater Res 1995;29:1215-21.

18. Sofia S, McCarthy MB, Gronowicz G, Kaplan DL. Functionalized silk-based biomaterials for bone formation. J Biomed Mater Res 2001; 54:139-48.

19. Okabe M, Ikawa M, Kominami K, Nakanishi T, Nishimune Y. 'Green mice' as a source of ubiquitous green cells. FEBS Lett 1997;407:313-9.

20. Sata M, Saiura A, Kunisato A, Tojo A, Okada S, Tokuhisa T, et al. Hematopoietic stem cells differentiate into vascular cells that participate in the pathogenesis of atherosclerosis. Nat Med 2002;8:403-9.

21. Fukuda D, Sata M, Ishizaka N, Nagai R. Critical role of bone marrow angiotensin II type 1 receptor in the pathogenesis of atherosclerosis in apolipoprotein E deficient mice. Arterioscler Thromb Vasc Biol 2008; 28:90-6.

22. Tanaka K, Sata M, Hirata Y, Nagai R. Diverse contribution of bone marrow cells to neointimal hyperplasia after mechanical vascular injuries. Circ Res 2003;93:783-90.

23. Sahara M, Sata M, Morita T, Nakamura K, Hirata Y, Nagai R. Diverse contribution of bone marrow-derived cells to vascular remodeling associated with pulmonary arterial hypertension and arterial neointimal formation. Circulation 2007;115:509-17.

24. Grzesiak JJ, Pierschbacher MD, Amodeo MF, Malaney TI, Glass JR. Enhancement of cell interactions with collagen/glycosaminoglycan matrices by RGD derivatization. Biomaterials 1997;18:1625-32.

25. He H, Shirota T, Yasui H, Matsuda T. Canine endothelial progenitor cell-lined hybrid vascular graft with nonthrombogenic potential. J Thorac Cardiovasc Surg 2003;126:455-64.

26. Kaushal S, Amiel GE, Guleserian KJ, Shapira OM, Perry T, Sutherland FW, et al. Functional small-diameter neovessels created using endothelial progenitor cells expanded ex vivo. Nat Med 2001;7:1035-40.

27. Matsumura G, Hibino N, Ikada Y, Kurosawa H, Shin'oka T. Successful application of tissue engineered vascular autografts: clinical experience. Biomaterials 2003;24:2303-8.

28. Moriya M, Roschzttardtz F, Nakahara Y, Saito H, Masubuchi Y, Asakura T. Rheological properties of native silk fibroins from domestic and wild silkworms, and flow analysis in each spinneret by a finite element method. Biomacromolecules 2009;10:929-35.

29. Zhao C, Yao J, Masuda H, Kishore R, Asakura T. Structural characterization and artificial fiber formation of Bombyx mori silk fibroin in hexafluoro-iso-propanol solvent system. Biopolymers 2003;69:253-9.

30. Setzen G, Williams EF 3rd. Tissue response to suture materials implanted subcutaneously in a rabbit model. Plast Reconstr Surg 1997;100:1788-95.

31. Bucknall TE, Teare L, Ellis H. The choice of a suture to close abdominal incisions. Eur Surg Res 1983;15:59-66.

32. Sahara M, Sata M, Matsuzaki Y, Tanaka K, Morita T, Hirata Y, et al. Comparison of various bone marrow fractions in the ability to participate in vascular remodeling after mechanical injury. Stem Cells 2005; 23:874-8.

33. Hillebrands JL, Klatter FA, van Dijk WD, Rozing J. Bone marrow does not contribute substantially to endothelial-cell replacement in transplant arteriosclerosis. Nat Med 2002;8:194-5.

34. Hu Y, Davison F, Ludewig B, Erdel M, Mayr M, Url M, et al. Smooth muscle cells in transplant atherosclerotic lesions are originated from recipients, but not bone marrow progenitor cells. Circulation 2002; 106:1834-9.

35. Fukuda D, Sata M, Tanaka K, Nagai R. Potent inhibitory effect of sirolimus on circulating vascular progenitor cells. Circulation 2005; 111:926-31.

36. Simper D, Stalboerger PG, Panetta CJ, Wang S, Caplice NM. Smooth muscle progenitor cells in human blood. Circulation 2002;106:1199-204.

37. Bocan TM. Animal models of atherosclerosis and interpretation of drug intervention studies. Curr Pharm Des 1998;4:37-52.

38. Torikai K, Ichikawa H, Hirakawa K, Matsumiya G, Kuratani T, Iwai S, et al. A self-renewing, tissue-engineered vascular graft for arterial reconstruction. J Thorac Cardiovasc Surg 2008;136:37-45, e1.